

1 **Paraglacial slope instability in Scottish fjords: examples from Little Loch Broom, NW**

2 **Scotland**

3

4 Martyn Stoker^{1*}, Charles Wilson^{2,3}, John Howe², Tom Bradwell¹ & David Long¹

5

6 ¹*British Geological Survey, West Mains Road, Edinburgh, EH9 3LA*

7 ²*Scottish Association for Marine Science, Oban, Argyll, PA37 1QA, UK*

8 ³*Department of Earth Sciences, Durham University, Durham, DH1 3LE, UK*

9 **Corresponding author (M Stoker): (email: mss@bgs.ac.uk)*

10

11 Number of words: 7,160 (excluding references and captions)

12 Abbreviated title: Slope instability in Scottish Fjords

13 Keywords: Fjord; Little Loch Broom; NW Scotland; Mass Failure

14

15 **Abstract**

16

17 Lateglacial–Holocene fjord sediments in Little Loch Broom preserve evidence of extensive slope

18 instability. The major area of reworking is in the outer loch and mid-loch sill region where ice-

19 contact/ice-proximal deposits of the Lateglacial Assynt Glacigenic Formation have been

20 disrupted by sliding and mass flow processes linked to the Little Loch Broom Slide Complex and

21 the adjacent Badcaul Slide. Mass failure was instigated about 14–13 ka BP, and is probably the

22 response of the landscape to deglaciation immediately following the removal of ice support

23 during glacial retreat. An initial phase of translational sliding was followed by rotational sliding,

24 as revealed by the superimposition of scalloped-shaped slumps on a larger-scale rectilinear
25 pattern of failure. Paraglacial landscape readjustment may have also been enhanced by episodic
26 seismic activity linked to glacio-isostatic unloading. In the inner fjord, evidence of Holocene
27 mass failure includes the Ardessie debris lobe and a discrete intact slide block preserved within
28 the postglacial basinal deposits. The former is a localised accumulation linked to a fluvial
29 catchment on the adjacent An Teallach massif. These mass transport deposits may represent an
30 ongoing response to paraglacial processes, albeit much reduced (relative to the major slides) in
31 terms of sediment supply to the fjord.

32

33 **Introduction**

34

35 It is well established that fjords are areas of major landslide activity due to their steep lateral
36 slopes, characteristically high rates of sedimentation, and commonly exceptional rates of isostatic
37 uplift (Syvitski & Shaw 1995; Hampton *et al.* 1996). These factors make them ideal
38 environments for all kinds of sediment deformation, be it due to gravitational reworking of the
39 rapidly accumulating deposits, fluid flow or to external stimuli, such as earthquakes. Examples of
40 sediment slides, slumps, and extensional and compressional deformation structures are to be
41 found in fjords worldwide, including Canada (Syvitski & Hein 1991), East Greenland
42 (Whittington & Niessen 1997; Niessen & Whittington 1997) and Norway (Aarseth *et al.* 1989;
43 Hjelstuen *et al.* 2009).

44

45 Scotland's fjords are no exception. Recent work in the Summer Isles region of NW Scotland
46 (Fig. 1) has identified an up to 100 m thick sequence of fjord sediments, which was rapidly

47 deposited during the landward retreat of the ice margin from the Summer Isles into the present-
48 day sea lochs of Loch Broom and Little Loch Broom (Stoker *et al.* in press). Swath bathymetric
49 imagery, high-resolution seismic reflection profiles and sediment core data have shown that mass
50 failure is pervasive throughout the Summer Isles region. Regional mapping has demonstrated that
51 early, post-depositional deformation in and around Loch Broom, including the Cadail Slide (Fig.
52 1), occurred during the Lateglacial interval (Stoker *et al.* 2006, in press; Stoker & Bradwell
53 2009). In this paper we focus on one of the largest areas of submarine mass failure yet to be
54 identified in nearshore UK waters – herein referred to as the Little Loch Broom Slide Complex
55 (Fig. 1). We also describe more localised features of instability in the inner part of Little Loch
56 Broom, including the Badcaul Slide and the Ardessie debris lobe; the latter most probably a
57 Holocene feature. We use geophysical and geological data to describe the style of the instability
58 and the nature of the resulting sediments, as well as to provide constraints on the timing of
59 failure. Considered together with the regional pattern of neotectonic deformation, the
60 development of the Little Loch Broom Slide Complex and adjacent mass failures may provide
61 clues as to the stability of the deglaciating Scottish hinterland during the Lateglacial–Holocene
62 interval.

63

64 **Regional Setting**

65

66 Little Loch Broom is a NW trending sea loch situated approximately 10 km west of Ullapool
67 (Fig. 1). The flanks of the loch are characterised by rugged headlands backed by mountains, such
68 as An Teallach to the south, and Beinn Ghoblach to the north. The loch is 12 km long, 0.5 to 2.0
69 km wide, and is divided more or less at its mid-point into inner and outer basins by a mid-loch

70 sill (~25 m below sea level). The deepest part of the loch is the inner basin (119 m), while the
71 outer basin reaches a maximum depth of 65 m (Stoker *et al.* 2006). Slope angles are also greater
72 in the inner loch (locally >50°) compared to the outer loch (locally up to 25°). No detailed
73 hydrographic survey from Little Loch Broom has been published; however, the Scottish
74 Environmental Protection Agency site data report for the loch (SEPA 2006) states that it is
75 protected from SW winds, but exposed to winds blowing from the NW. Heath *et al.* (2000) used
76 data from Lee and Ramster's *Atlas of the Sea* (1981) to estimate a mean spring tidal current of 1-
77 2 ms⁻¹ in both Loch Broom and Little Loch Broom. The approximate average flushing time for
78 the whole loch is 7 days, although the deeper basins take longer, and freshwater input is generally
79 low (SEPA 2006).

80
81 The depth to bedrock in Little Loch Broom is locally up to 160 m (maximum) below OD, in the
82 inner loch. The bedrock geology is dominated by Neoproterozoic Torridonian sandstone with
83 sporadic inliers of Archaean gneiss near the mouth of the loch. The orientation of the loch is
84 structurally controlled by a fault that trends along the length of Little Loch Broom (Fig. 1).
85 Significant NE trending structures in the area include the Moine Thrust and the Coigach fault.

86
87 The regional glacial geology of the Summer Isles area is summarised in Figure 2 and Table 1; for
88 details see Stoker *et al.* in press. All dates have been calibrated (Fairbanks *et al.* 2005) and are
89 expressed as calendar years (ka BP). The major part of the succession records a time-
90 transgressive landward retreat of the Lateglacial ice-sheet margin from The Minch, across the
91 Summer Isles, back to the sea lochs of Loch Broom and Little Loch Broom. The deposition of
92 ice-contact to ice proximal glacimarine and ice-distal glacimarine facies, assigned to the Assynt

93 Glacigenic and Annat Bay Formations, respectively, comprise the bulk of the sediment infilling
94 the fjord region. Cosmogenic-isotope surface-exposure ages of boulders from onshore moraines
95 within the Assynt Glacigenic Formation, combined with AMS radiocarbon dating of marine
96 shells from, and micropalaeontological analysis of, both the Assynt Glacigenic and Annat Bay
97 Formations in offshore sediment cores all suggest that these units were deposited largely between
98 about 14 and 13 ka BP, i.e. during the Lateglacial Interstadial (Bradwell *et al.* 2008; Stoker *et al.*
99 in press). In Loch Broom, there is evidence of late-stage oscillation of outlet glacier lobes back
100 into the fjord; this correlates with several discrete Late-stage members of the Assynt Glacigenic
101 Formation. An associated series of large fan-deltas comprise the Ullapool Gravel Formation,
102 which is sandwiched between these Late-stage members. As the fjord gradually became ice free,
103 the Outer and Inner Loch Broom shell beds accumulated as a time-transgressive deposit on the
104 floor of the fjord. The Inner Loch Broom shell bed is overlain by glacial diamicton belonging to
105 one of the Late-stage members of the Assynt Glacigenic Formation in the inner loch. This
106 relationship provides an age constraint of <13 ka BP for the late-stage ice-margin oscillation
107 within the inner fjord. A discrete lithogenetic unit, informally named the ‘Late-stage debris
108 flows’, occurs sporadically throughout the Summer Isles region. This unit post-dates the Assynt
109 Glacigenic and Annat Bay Formations, but pre-dates the Summer Isles Formation, which forms a
110 cover of Holocene marine sediments deposited after about 8 ka BP.

111
112 The Assynt Glacigenic, Annat Bay and Summer Isles Formations, together with the Late-stage
113 debris flow lithogenetic unit, have all been mapped in and around the inner part of Little Loch
114 Broom (Fig. 3). In contrast, the shallower, outer part of the loch is dominated almost completely
115 by the Assynt Glacigenic Formation, and its reworked upper component assigned to the

116 Rireavach Member; these units are overlain by a seismically unresolvable Holocene veneer
117 (Stoker *et al.* in press) (Figs 2 & 3). The mid-loch sill that separates the inner and outer lochs is
118 formed by a coincidence of a bedrock high and a major moraine ridge associated with the Assynt
119 Glacigenic Formation. Other prominent moraine ridges also belonging to this unit are preserved
120 on sills at the mouth (outer loch moraine) and near the head (inner loch moraine) of the loch.
121 From a stratigraphic perspective, the Rireavach Member defines the reworked extent of the
122 Assynt Glacigenic Formation within the confines of the Little Loch Broom Slide Complex.
123 Additional mass transport deposits are associated with the Late-stage debris flow unit, linked to
124 the Badcaul Slide, and with the Summer Isles Formation, including the Ardessie debris lobe.

125

126 **Methods**

127

128 This study combines geophysical and geological data collected by the British Geological Survey
129 (BGS) and the Scottish Association for Marine Science (SAMS) in the Summer Isles region
130 between 2005 and 2007. A marine geophysical survey of the Summer Isles region, including
131 Little Loch Broom, was undertaken in July 2005, and acquired multibeam swath bathymetry and
132 high-resolution seismic reflection data (Stoker *et al.* 2006). Bathymetric data were acquired using
133 a GeoSwath system operating at 125 kHz, mounted on a retractable bow pole on the *R/V*
134 *Calanus*. Swath survey lines were traversed at a spacing of 200 m, thereby enabling swath
135 overlap and full coverage bathymetry across an area of 225 km². The data were collected on a
136 GeoSwath computer with post-acquisition processing carried out on a separate workstation.
137 Output was in the form of xyz data with a typical grid spacing of 3 m. The grid was converted
138 into a depth-coloured shaded-relief image using Fledermaus (processing and visualisation

139 software). The shaded-relief image of the study area is shown in Figure 4. The seismic reflection
140 data were acquired using a BGS-owned Applied Acoustics surface-towed boomer and
141 hydrophone. Fifty-seven boomer profiles (a total length of about 235 km) were collected across
142 the region, including twelve profiles specifically acquired in Little Loch Broom. The data were
143 recorded and processed (Time Varied Gain, Bandpass Filter 800–200 Hz) on a CODA DA200
144 seismic acquisition system and output as SEG-Y and TIFF format. Further technical details of the
145 geophysical data collection are outlined in Stoker *et al.* (2006).

146
147 On the basis of regional measurements of superficial sediments offshore Scotland, sound
148 velocities in the fjord sediment fill are taken to be in the range of 1500–2000 ms⁻¹ depending
149 upon their composition and degree of induration (McQuillin & Arduş 1977; Stoker *et al.* 1994).
150 In this paper, the conversion of sub-bottom depths from milliseconds to metres has been
151 generally taken as a maximum estimate (e.g. 20 ms two-way travel time (TWTT) ≤20 m) of
152 sediment thickness. The relief of features with expression at the sea bed is based on the sound
153 velocity in water of 1450 ms⁻¹ (Hamilton 1985).

154
155 Geological calibration of the geophysical data was established using SAMS gravity cores GC087,
156 088, 092, 093, 112, 113, 115, 120 and 122, and BGS vibrocore 57-06/286 (a re-occupation of site
157 GC122) (Fig. 4). The SAMS cores were collected from the *M/V Calanus* in August 2006,
158 whereas the BGS core was collected in September 2007, using the *R/V James Cook*. Stratigraphic
159 correlation of these cores is based on a regional study of all cores collected in the Summer Isles
160 region (a total of 50 sample stations), which is detailed in Stoker *et al.* (in press). The lithology of
161 the cores is summarised in Table 2.

162

163 **Indicators of instability in outer Little Loch Broom**

164

165 *Little Loch Broom Slide Complex*

166

167 The Little Loch Broom Slide Complex extends between the mid- and outer loch moraine/bedrock
168 sills (Figs 3–5a). In this area, the maximum water depth is approximately 75 m. The sea bed in
169 the centre of the outer loch is flat, whereas much of the rest of the basin is characterised by
170 undulating bathymetry and an irregular, scalloped margin (Fig. 5a). On this basis, three main
171 areas of sliding have been identified, designated the Rireavach, Carnach and Scoraig slides, with
172 a further area of debris lobes offshore Corran Scoraig, near the outer sill. The morphology of
173 these features is detailed below, together with the resultant deposits, which collectively comprise
174 the Rireavach Member (Assynt Glacigenic Formation).

175

176 *Rireavach Slide.* This slide is the largest feature identified in Little Loch Broom, and has
177 affected an area of the sea bed about 1–2 km² (Fig. 5a). Three distinct scarp surfaces (1–3) are
178 observed on the swath image, confirmed by their correlation with the boomer profile that
179 transects the slide (Fig. 3b). The most distinctive backscarp (1) displays a generally rectilinear
180 margin, at a water depth of about 35 to 40 m, that can be traced around the entire area of the
181 slide, a distance of about 4 km, and defines two main erosional hollows or re-entrants: a northern
182 one (NR) constrained by the side of the loch, and an eastern one (ER) constrained by the
183 morainic rampart that forms the mid-loch sill. These re-entrants indicate that material has been
184 displaced into the basin in both southerly (NR) and westerly (ER) directions. However, the

185 rectilinear shape of the scarp appears to have been modified by smaller scale (≤ 200 m), curved or
186 scalloped indentations that impart an irregularity to the backscarp. The southern wall of the loch
187 appears to have remained linear, steep and less obviously affected by sliding. Scarps 1–3 (in the
188 eastern re-entrant) range from 7 to 15 m high, with slope angles between 7° and 15° . They
189 display sub-planar to predominantly curved, concave-up, profiles. Distinct terraces occur between
190 scarps 1–2 and 2–3, at water depths of about 55 m and 65 m, respectively. The present-day basin
191 floor, at the foot of scarp 3 is at about 75 m water depth. Along the western edge of the northern
192 re-entrant (NR), the delineation of the separate scarps is less clear and a single scarp is present,
193 with an upper headwall limit at 30 to 35 m water depth, a vertical relief of 35 m and a slope angle
194 up to 10° . In Figure 3b, the seismic profile shows the basin floor to be slightly undulatory; a
195 characteristic also observed on the swath image (Fig. 5a).

196

197 *Carnach Slide.* The Carnach Slide forms a much smaller sea bed hollow on the northern slope
198 of the loch, between about 35 and 55 m water depth (Fig. 5a). It occupies an area of about 0.05
199 km^2 , has displaced sediment to a depth of about 5 m below sea bed, displays a curved, concave-
200 up, profile, with a maximum backscarp slope angle up to about 13° . Downslope of the scar, an
201 equivalent area of seabed is raised ~ 1 – 2 m (convex-up) above the adjacent sea floor for a
202 distance of up to 300m from the foot of the scar. At least two separate lobes are identified from
203 the swath image, which represent material derived from the slide scar.

204

205 *Scoraig Slide.* The Scoraig Slide is expressed as a discrete crenulate scar that broadly
206 parallels the northern slope of the loch for about 500 m (Fig. 5a). The slide scar covers an area
207 of about 0.25 km^2 , and is cut into the slope between about 30 and 65 m water depth. It displays

208 a curved, concave-up, slide surface profile, with a maximum backscarp angle up to 18°. Several
209 debris lobes are visible at the base of the scar, raised ~1-2 m above the sea bed, and extending
210 250–300 m into the basin, and up to 600 m along the strike of the basin.

211

212 *Debris lobes offshore Corran Scoraig.* Further NW along the northern flank of the outer loch
213 a series of less well-defined crenulations and hollows are visible on the swath image, some of
214 which have a gully-like appearance, up to 10 m deep and several tens of metres wide (Fig. 5a).
215 A series of overlapping debris lobes up to 4 m in relief and up to several hundred metres wide,
216 are found towards the base of the slope forming a package that extends for up to 1.3 km along
217 the axis of the basin. There may also be some input from the southern slope, though the swath
218 image is increasingly restricted (due to operational constraints) in extent near the mouth of the
219 loch. On both the swath image and the seismic profile data, the basin floor topography is
220 hummocky.

221

222 *Rireavach Member (slide complex deposits).* The Rireavach Member of the Assynt Glacigenic
223 Formation forms a discrete fjord slope to basin-floor package of mass transport deposits derived
224 from multiple slide sources. It has accumulated below about 30 m water depth, the approximate
225 upper bounding limit of the headwalls of the slides. On seismic profiles, it displays an irregular,
226 hummocky, sheet-like geometry, up to 12 m thick. In Figure 3, the base of the Rireavach Member
227 (the base of the slide complex) is clearly depicted by the truncation of acoustically layered strata
228 in the underlying, undisturbed deposits of the Assynt Glacigenic Formation. Internally, the mass
229 transport deposits display a predominantly chaotic internal reflection configuration; however,

230 sporadic subhorizontal reflections are locally observed, particularly in the area of the Rireavach
231 Slide and within the pile of debris lobes off Corran Scoraig, near the mouth of the outer loch.
232

233 The deposits of the Rireavach Member have been sampled at three sites: GC087, GC119 and
234 GC122 (57-06/286). All three cores are from the basin floor (Figs 4 & 5), and all recovered
235 different lithologies (Table 2). Deposits of the Rireavach Slide were tested by core GC087, which
236 recovered 0.62 m of colour laminated silty clay overlying a 0.14 m thick bed of shelly, gravelly,
237 sandy mud, in turn overlying homogeneous clay and silty clay. The contacts between all three
238 beds are sharp, and the laminated clay displays angular discordance with the underlying bed. In
239 Figure 6a, the laminations are clearly observed to be inclined, relative to the underlying bed of
240 sandy mud, and partially disrupted and offset along small faults. The laminated clay is in sharp
241 contact with the overlying Holocene unit, the base of which is marked by a gravelly and shelly
242 lag deposit (Fig. 4). Core GC119 is located on the edge of the debris lobes derived from the
243 Scoraig Slide, where the Rireavach Member contained a 0.2 m thick sandy bed overlying 0.69 m
244 of slightly sandy clay. Discrete patches of lithic grains are scattered throughout the clay and
245 possibly represent coarser, matrix-supported intraclasts. There is a sharp contact with the
246 overlying Holocene sandy mud. Cores GC122 and 57-06/286 tested the debris lobes off Corran
247 Scoraig and recovered 2.57 m of massive, compact, reddish brown gravelly sand, the top of
248 which is reworked and overlain by a veneer of Holocene muddy sand.
249

250 *Pre-slide deposits (Assynt Glacigenic Formation).* Cores GC112/113 and 120 are located in the
251 slide scar region of the Rireavach and Carnach slides, respectively (Fig. 4). They both recovered
252 homogeneous to colour laminated mud and clay with sporadic pebbles, shelly material and thin

253 beds of muddy sand. The same lithofacies was also present in cores GC093 and GC115, which
254 penetrated the Assynt Glacigenic Formation outside of the slide complex; GC093 is located
255 adjacent to the major moraine on the mid-loch sill. In all of these cores, this lithofacies is sharply
256 overlain by a Holocene shelly and gravelly lag deposit. The colour laminated mud and clay is
257 distinctive of the Assynt Glacigenic Formation throughout the Summer Isles region (Stoker *et al.*
258 in press), and in Little Loch Broom the sediments in these cores are regarded as being part of the
259 undisturbed, pre-sliding, fjord section.

260

261 **Indicators of instability in inner Little Loch Broom**

262

263 The fjord infill succession in inner Little Loch Broom is far less disturbed in comparison to the
264 outer loch; this is most probably a function of the steeper sides of the inner loch precluding the
265 accumulation of significant sidewall deposits. However, there are several indicators of instability,
266 specifically the Badcaul Slide and associated Late-stage debris flow unit, together with the
267 Ardessie debris lobe and a discrete slide deposit in core GC088, both of which are associated
268 with the Holocene Summer Isles Formation.

269

270 *Badcaul Slide*

271

272 The term Badcaul Slide is herein utilised in reference to a 1-km² diffuse zone of disturbance on
273 the SE side of the mid-loch sill that has affected the Assynt Glacigenic Formation (Figs 3 & 7).
274 The swath image displays a number of terraces with irregular, scalloped, backscarps stepping
275 down into the inner loch. However, the most distinctive terrace, which occurs on the main part of

276 the sill at about 60 m water depth, displays a rectilinear shape up to 800 m wide and backed by a
277 headwall with a slope angle up to 15°, and which is traced for 1.5–2 km. A series of narrower
278 (about 50 m wide) terraces occur between about 70 and 90 m water depth (Fig. 7). The narrower
279 terraces coincide with what appear to be several slide and/or slump blocks observed on the
280 seismic profile. The internal seismic reflection configuration of the Assynt Glacigenic Formation
281 on this part of the fjord wall is mostly structureless to irregular and chaotic, but with
282 discontinuous sub-planar reflecting surfaces dipping into the basin that impart a general large-
283 scale tabular structure to the depositional package (Fig. 7b). Gently curved, smaller scale,
284 concave-up, slide surfaces are also observed within the upper part of the slide package, and,
285 where bedding is observed, some rotation of reflections (including the sea bed) into the slope is
286 locally evident (Fig. 7b: upper inset). At the base of the slope, the sea bed occurs at 110 m water
287 depth and is characterised by a hummocky morphology that becomes smoother into the basin.
288 The seismic profile shows that this reflects a large debris lobe that has accumulated at the base of
289 the slope, and which becomes progressively buried beneath younger sediments into the basin
290 (Figs 3 & 7b). The debris lobe is up to 10–12 m thick, is lensoid in shape with a chaotic internal
291 reflection configuration, and can be traced for about 800 m along the line of the profile (Fig. 7b:
292 lower inset). This deposit forms part of the Late-stage debris flow lithogenetic unit of Stoker *et*
293 *al.* (in press). The overlying deposits belong to the Holocene Summer Isles Formation.
294
295 The debris lobe has been sampled by core GC092, which contained 1.5 m of homogeneous silty
296 clay of the Summer Isles Formation, with a slightly sandy base, sharply overlying 0.6 m of
297 interbedded silty clay and muddy sand of the Late-stage debris flow unit. Most of the latter
298 deposit is folded with recumbent isoclinal folds depicted by the paler sandy beds in Figure 6b. It

299 is unclear whether or not the basal sandy bed in the core is part of the deformed section; its
300 contact with the overlying interbedded section is sharp.

301

302 *Ardessie debris lobe*

303

304 The Ardessie debris lobe has been identified on the southern flank of inner Little Loch Broom,
305 immediately offshore Ardessie, at a water depth of 75–80 m (Figs 4 & 5b). The swath image
306 shows several gullies, 2–5m deep and 20–50m wide, eroded into the side of the fjord, on a slope
307 angle of 13°. At the base of the slope, a debris lobe is clearly observed at sea bed, with a convex-
308 up relief of up to 2m above the surrounding sea bed and covering an area of approximately 0.2
309 km². Traced landward, the gullies trend back towards the coastline at the point where the Allt
310 Airdeasaidh drains into the loch. This stream and its tributaries drain part of the An Teallach
311 massif (Fig. 4), and have a catchment area of approximately 10km².

312

313 The debris lobe is similarly well imaged on seismic profile data, which show a discrete lobe at
314 the sea bed with a double hump that may be indicative of several smaller component lobes. The
315 hummocky nature of the sea bed associated with the debris lobe contrasts with the generally
316 smoother morphology of the basin floor (Fig. 5b). The seismic profile also reveals an acoustically
317 structureless internal reflection configuration, and that the debris lobe overlies the bulk of the
318 basinal deposits associated with the Summer Isles Formation. In contrast to the Badcaul Slide,
319 there is no indication that the debris lobe is buried beneath any younger sediment (within seismic
320 resolution: ~0.5 m). A linear trail of pockmarks, which is associated with shallow gas in the
321 basin, appears to follow the course of a buried, former meltwater channel that retains expression

322 at the sea bed (Fig. 5b); however, it is unclear whether or not the debris lobe pre- or post-dates
323 pockmark formation. Although there are no core data available, the seismic stratigraphy indicates
324 that this is a Holocene deposit.

325

326 *Core GC088 (Summer Isles Formation)*

327

328 Core GC088 is located close to the southern slope of the inner loch, at a water depth of 102 m.

329 The core penetrated 2.88 m into the Summer Isles Formation, and recovered predominantly soft,
330 sticky, homogeneous, mottled silty clay. The seismic profile at the core site shows an undisturbed
331 acoustically bedded character; however, the core revealed a discrete bed of folded laminated clay
332 between 2.32 and 2.75 m (Fig. 6c) in contrast to the enclosing sediment. The deformed
333 lamination reveals recumbent folds showing varying degrees of complexity in fold pattern, from
334 symmetrical to asymmetrical isoclinal folds. The contact of the deformed bed with the underlying
335 homogeneous silty clay is sharp; the contact with the overlying bed also appears to be sharp,
336 though there may be some disruption of the top of the bed due to subsequent bioturbation or
337 erosion. It seems probable that this is a discrete bed of deformed clay incorporated within the
338 more typical basinal silty clay of the Summer Isles Formation.

339

340 **Interpretation and discussion**

341

342 *Types of mass transport*

343

344 The swath bathymetric, seismic reflection and core data provide unambiguous evidence for
345 widespread slope instability within Little Loch Broom, and two main types of mass transport
346 process can be identified: 1) sliding; and, 2) mass flow (Table 3). These processes are not
347 mutually exclusive, as the mass flow deposits are commonly sourced from the adjacent slides,
348 e.g. Carnach Slide (Fig. 5a), though the Ardessie debris lobe is a more discrete feature linked to a
349 series of slope gullies. The main characteristics of these two types of mass transport process are
350 described below, and summarised in Table 3:

351

352 *Slides:* A major characteristic of the slide failure surfaces found within the Little Loch Broom
353 Slide Complex, as well as the Badcaul Slide, is their curved, concave-up, profile, the morphology
354 of which is enhanced on the swath bathymetric image by the scallop shaped nature of the scarps
355 (Figs 5 & 7). Tilting of bedding is locally observed in the upper part of the Badcaul Slide mass
356 transport deposit, where bedding is rotated into the failure surfaces (Fig. 7b: upper inset).
357 However, the swath bathymetry also reveals that this irregular pattern of scarps is superimposed
358 on a larger-scale rectilinear pattern of failure, as indicated by both the northern and eastern re-
359 entrants of the Rireavach Slide, as well as the shallow part of the Badcaul Slide on the mid-loch
360 sill. Slides on curved surfaces are classified as slumps, whereby failure is accompanied by
361 rotation; in contrast, planar slides are classified as glides, with failure facilitated by translation
362 (Nardin *et al.* 1979; Cook *et al.* 1982; Mulder & Cochonat 1996). Our data suggest that both
363 translational and rotational sliding have occurred in Little Loch Broom, the implications of which
364 in terms of release mechanisms and timing of mass movement are considered elsewhere in this
365 section.

366

367 Probable slide deposits were recovered in cores GC087 and GC088 from the Rireavach Member
368 and Summer Isles Formation, respectively, which proved beds of deformed laminated clay in
369 sharp contact with undeformed beds (Figs 4 & 6a, c). The deformed laminations range from
370 gently inclined (core GC087) to recumbent and isoclinally folded (core GC088). The abrupt
371 contact with undeformed beds suggests that these beds represent discrete blocks that have moved
372 downslope. Despite some internal deformation they have retained an internal coherency in that
373 continuous laminations are still preserved. Deformation of the sediment may have begun as
374 creep, which, as gravitational stresses increased, may have ultimately failed as an intact block
375 (Syvitski & Shaw 1995). Comparable structures have been described from slide deposits cored on
376 the continental slope offshore Nova Scotia and elsewhere (Cook *et al.* 1982; Jenner *et al.* 2007),
377 and are commonly attributed to elastic mechanical behaviour of the sediment during submarine
378 slope failure (Nardin *et al.* 1979). As core GC087 did not penetrate the entire mass transport
379 deposit associated with the Rireavach Slide, the possibility that this bed represents a rafted block
380 within a debris flow cannot be discounted.

381

382 *Mass flows:* Mounded, lensoid and lobate packages of sediment form the predominant basin
383 floor deposit associated with the Little Loch Broom Slide Complex and the Badcaul Slide, as
384 well as the more discrete Ardessie debris lobe. This depositional morphology, combined with a
385 general lack of internal reflectors, is characteristic of mass flow deposits, whereby the absence of
386 internal structure is commonly related to deformational homogenisation of the sediment mass
387 during submarine slope failure (Nardin *et al.* 1979). The swath bathymetry shows clearly that the
388 Scoraig and Carnach debris lobes are derived from the adjacent slides, whereas several failure
389 surfaces have contributed to the accumulation of the basinal mass flow package associated with

390 the Rireavach Slide (Fig. 5a). The Late-stage debris flow unit at the foot of the Badcaul Slide is
391 sourced from the Badcaul Slide; the deposit gradually thinning into the basin (Fig. 7b). By way
392 of contrast, the Ardessie debris lobe is localised at the base of a series of erosional gulleys that
393 transect the adjacent slope (Fig. 5b). The hummocky surface of many of these mass flow
394 packages, as imaged on swath bathymetry or seismic profiles, suggests that each of the main
395 packages, which may extend >1 km across the basin floor, consists of an amalgamation of
396 smaller, stacked flows, e.g. the Scoraig and Ardessie debris lobes, that may be up to a maximum
397 of a few hundred metres in width.

398
399 The core data suggest that a number of different mass flow processes may have operated during
400 slope failure. The occurrence of a clay bed with matrix-supported intraclasts in core GC119, from
401 a mass flow lobe at the base of the Scoraig Slide (Fig. 4), is consistent with muddy debris-flow
402 deposition, which is associated with plastic mechanical behaviour whereby the strength of the
403 flow is principally a result of cohesion due to the clay content (Nardin *et al.* 1979; Mulder &
404 Cochonat 1996). In contrast, the massive gravelly sand recovered in cores GC122 and 57-06/286,
405 from the area of debris lobes offshore Corran Scoraig (Fig. 4), may be more characteristic of a
406 grain flow (Lowe 1982) or a sandy debris flow (Middleton 1967; Shanmugan 1996), whereby the
407 less cohesive sandy material is supported by dispersive pressure, thus exhibiting pseudo-plastic
408 flow, and deposited by ‘freezing’. Although, rapid mass deposition from a high-concentration
409 turbidity current – the Bouma A division – cannot be discounted, there is no evidence in the cores
410 for grading, which is commonly a defining structure in such deposits (Pickering *et al.* 1989;
411 Shanmugan 1996). Whereas debris flows can be initiated and moved along low-angle slopes,
412 grain flows usually require steep slopes for initiation and sustained downslope movement (Nardin

413 *et al.* 1979). All of these sediment types have been described in association with mass flow
414 processes from continental slopes and fjords (Cook *et al.* 1982; Syvitski & Hein, 1991; Jenner *et*
415 *al.* 2007). In core GC092, from the Late-stage debris flow unit, a deformed, folded bed was
416 present at the top of the mass flow lobe, underlain by a sandy bed. The deformed bed is more
417 typical of a slide block, as described above, and in this setting it may represent a rafted block
418 incorporated within the mass flow. Unfortunately, no core data are available at this time from the
419 Ardessie debris lobe. However, its association with erosional gullies implies some kind of
420 sediment gravity flow process linked to the formation of the gullies. On continental slopes, such
421 gullies are commonly associated with turbidity currents (Pickering *et al.* 1989). In Little Loch
422 Broom, the Ardessie debris lobe and associated gullies appear to represent the sink for part of the
423 fluvial catchment area on the northern slope of An Teallach drained by the Allt Airdeasaidh (Fig.
424 4); this potential linkage is further discussed below.

425

426 *Timing of mass failure*

427

428 A significant phase of mass failure is reported from elsewhere within the Summer Isles region
429 between about 14 and 13 ka BP, including the Cadail Slide in the North Annat Basin, and
430 slumping of basinal sediments in outer Loch Broom (Stoker & Bradwell 2009; Stoker *et al.* in
431 press) (Fig. 1). Seismic-stratigraphy indicates that the Cadail Slide, which also deformed
432 sediments of the Assynt Glacigenic Formation, occurred immediately prior to the deposition of
433 the glacimarine Annat Bay Formation in the North Annat Basin. A similar relationship is
434 observed in this study from the Badcaul Slide, where the main package of mass transport deposits
435 (of the Assynt Glacigenic Formation) is overlapped by the Annat Bay Formation (Figs 3b & 7b).

436 However, the Late-stage debris flow unit, also linked to the Badcaul Slide, overlies the Annat
437 Bay Formation, but is itself overlapped by the Summer Isles Formation. This stratigraphical
438 relationship supports strongly the idea that mass failure in Little Loch Broom (including the Little
439 Loch Broom Slide Complex) was initiated during the Lateglacial interval. It also suggests that
440 large-scale mass flow processes persisted for some time after the deposition of the Annat Bay
441 Formation, but are no younger than about 8 ka BP, the onset of deposition of the Summer Isles
442 Formation (Stoker *et al.* in press). A Holocene veneer also overlies the slide and mass flow
443 deposits of the Rireavach Member in outer Little Loch Broom. In contrast, the Ardessie debris
444 lobe and the slide deposit in core GC088 are both part of the Summer Isles Formation, and thus
445 are of Holocene age. This suggests that discrete areas of mass failure have continued to develop
446 in Little Loch Broom within the postglacial interval.

447
448 *Triggering mechanism for mass failure, and implications for Lateglacial–Holocene instability in*
449 *the Summer Isles region*

450
451 When glacier ice occupies a fjord, subglacial sediment and morainic debris are deposited on
452 sidewalls, which are commonly very steep. However, during glacier retreat, such sediment-
453 mantled slopes become inherently unstable as they lose support during glacial downwasting
454 (Church & Ryder 1972; Ballantyne 2002; Powell 2005). Thus, sidewall sediment is prone to
455 failure by gravitational processes soon after the removal of glacier ice (Syvitski 1989; Syvitski &
456 Shaw 1995; Ballantyne 2002). The walls of Little Loch Broom are no exception; they are locally
457 very steep, exceeding 50° on the northern slope of the inner loch close to the mid-loch sill. The
458 triggering of mass failure in Little Loch Broom due to the removal of ice support is consistent

459 with a timing of failure during the Lateglacial interval – as the depositional environment changed
460 from an ice-contact/ice-proximal setting to an ice-distal setting. Arguably, the initial failure on
461 both the Rireavach and Badcaul slides was as rectilinear glide blocks that slid downslope. The
462 sub-planar, basinward-dipping reflections in the mass transport package of the Badcaul Slide
463 imply a tabular geometry to this sediment package. However, the rectilinear shape of these two
464 slides has been subsequently modified by numerous smaller-scale, scallop-shaped failures whose
465 curved surfaces and evidence of bed rotation indicate rotational sliding (slumps). This is also the
466 dominant style of the smaller Carnach and Scoraig slides.

467
468 The time-lag between large-scale slide initiation and subsequent modification by smaller-scale
469 slumps is unknown, though the available stratigraphic evidence that has been presented suggests
470 that it had mostly occurred before 8 ka BP. This scenario is consistent with the paraglacial
471 concept of Church & Ryder (1972), who emphasised the relatively rapid adjustment of
472 deglaciated landscapes to nonglacial conditions through the enhanced operation of a wide range
473 of processes, including slope failure and mass transport. This essentially involves the progressive
474 relaxation of unstable or metastable elements of the formerly glaciated landscape to a new, more
475 stable state (Ballantyne 2002). Although the reason for the change in the style of sliding is
476 unclear, we propose the following two-stage process: 1) the planar rupture surfaces associated
477 with the rectilinear slide blocks most likely follow weak bedding layers within the poorly
478 consolidated sediment pile, rendering them highly susceptible to gravity sliding in the early stage
479 of deglaciation of the fjord; 2) rotational sliding is less influenced by bedding – instead, it may
480 relate more to subsequent rupturing of the infill through fractures generated by stress relaxation
481 in the later stage of deglaciation.

482
483 The identification of mass transport deposits within the Summer Isles Formation in inner Little
484 Loch Broom indicates that paraglacial processes probably continued into the Holocene. The
485 relaxation of the landscape following a widespread glaciation can operate over timescales of
486 10^1 – 10^4 years, although the rate of sediment transfer is greatest immediately after deglaciation
487 and probably declines exponentially with time (Ballantyne 2002). On this basis, we infer that this
488 Little Loch Broom fjord region may still not have fully adjusted (in terms of sediment transfer) to
489 nonglacial conditions. In particular, the Ardessie debris lobe appears to be a localised,
490 anomalous, Holocene, seafloor sediment accumulation linked via a series of slope gullies to part
491 of the An Teallach drainage basin. We suggest that the source of the mass flow material is
492 reworked glacial deposits on the northern flank of the An Teallach massif, through fluvial
493 incision by the Allt Airdeassaidh and its tributaries (Fig. 4).

494
495 Paraglacial landscape readjustment may also have been enhanced by episodic seismic activity.
496 Mass failure linked to glacio-isostatic rebound is a well-established phenomenon along the
497 Atlantic continental margin of NW Europe. On the SW Norwegian margin, a detailed study of the
498 giant Storrega Slide concluded that a major seismic pulse most likely accompanied deglaciation
499 (Evans *et al.* 2002; Bryn *et al.* 2003; Haflidason *et al.* 2004). Differential rebound following ice
500 unloading is also known to reactivate pre-existing structural lineaments and bedrock weaknesses
501 as the new stress regime is accommodated, and enhanced neotectonic seismicity along the coastal
502 areas of northern, western and southeastern Norway is an established fact (Olesen *et al.* 2008). In
503 the UK, the earliest postglacial reactivation of pre-existing Caledonian and older lineaments is
504 known to have generated normal faulting with metre-scale displacement in the southern Sperrin

505 Mountains, in Northern Ireland (Knight 1999). Differential rebound and seismicity may also have
506 resulted in movement on faults, such as the Kinloch Hourn Fault, in western Scotland (Stewart *et*
507 *al.* 2001), and possibly caused liquefaction of lake sediments at Glen Roy, in Scotland (Ringrose
508 1989). Consequently, it seems probable that palaeoseismic activity was also occurring in the
509 Summer Isles region during Lateglacial–Holocene time. This hypothesis is strengthened when it
510 is noted that the west coast of Scotland, from Ullapool to Arran, continues to the present-day to
511 be a major focus for earthquakes (Musson 2003). Indeed, Stoker & Bradwell (2009) concluded
512 that earthquake activity was the most likely trigger of slumping and deformation of the basin-
513 floor fjord sediments in outer Loch Broom. It may be no coincidence that all three areas of large-
514 scale sediment deformation in the Summer Isles region (North Annat Basin, Loch Broom and
515 Little Loch Broom) are located along lines of NW trending faults (Fig. 1).

516

517 **Conclusions**

518

- 519 • Swath bathymetry, seismic reflection profiles and sediment core data have revealed evidence
520 of extensive slope instability within Lateglacial and Holocene sediments in Little Loch
521 Broom. The major area of reworking is in the outer loch where ice-contact/ice-proximal fjord
522 infill deposits of the Lateglacial Assynt Glacigenic Formation have been extensively
523 reworked by sliding and mass flow processes linked to the Little Loch Broom Slide Complex.
524 Collectively, this consists of the Rireavach, Carnach and Scoraig slides and associated mass
525 transport deposits – assigned to the Rireavach Member of the Assynt Glacigenic Formation.
526 In the inner loch, the Badcaul Slide has reworked the Assynt Glacigenic Formation on the
527 eastern flank of the mid-loch sill, and a major mass flow deposit at the foot of the slope is

528 assigned to the Late-stage debris flow lithogenetic unit. Elsewhere in the inner loch, localised
529 sliding and mass flow deposition, including the Ardessie debris lobe and an intact slide block
530 in core GC088, are preserved in the Holocene Summer Isles Formation.

531 • Regional stratigraphic and isotopic dating evidence suggest that the Little Loch Broom Slide
532 Complex and the Badcaul Slide were instigated between 14 and 13 ka BP, and that the bulk
533 of the mass failure activity had occurred prior to 8 ka BP. The Ardessie debris lobe and
534 GC088 slide-block deposit are both younger than 8 ka BP.

535 • The sea bed morphology and sub-bottom profiles suggest that both translational and
536 rotational sliding mechanisms were active in the generation of the Rireavach and Badcaul
537 slides; the superimposition of scalloped-shaped slumps on a larger-scale rectilinear pattern of
538 failure implies that an initial glide phase was superseded by rotational backwall failure. A
539 variety of associated mass transport deposits include intact blocks of laminated clay, and
540 mounded mass flow deposits (muddy debris-flow and sandy debris flow or grain-flow
541 deposits) preserved on the floor of the fjord. In contrast, the Holocene Ardessie debris lobe is
542 a localised, anomalous accumulation in the inner loch that appears to be fed by a series of
543 discrete slope gullies – downslope continuations of the Allt Airdeasaidh, which drains part of
544 the An Teallach massif. The intact Holocene slide block in core GC088 implies continuing,
545 albeit sporadic, post-glacial slide activity in the fjord.

546 • On the basis that the bulk of the mass failure in Little Loch Broom probably occurred
547 between about 14 and 8 ka BP, we infer that the major trigger of instability is probably the
548 response of the landscape to deglaciation, immediately following the retreat of the last ice
549 sheet. We further suggest that paraglacial landscape readjustment may have been enhanced in
550 this particular region by episodic seismic activity linked to glacio-isostatic unloading along

551 pre-existing geological faults. By way of contrast, the Holocene Ardessie debris lobe may
552 relate to erosion of the drift-mantled northern slopes of the An Teallach massif. This, together
553 with the slide block in core GC088, may represent an ongoing, albeit much reduced, response
554 to paraglacial processes in the fjords of NW Scotland.

555

556 **Acknowledgements**

557

558 The authors would like to thank the masters and crew of the *R/V Calanus* and *R/V James Cook*
559 for their skill and assistance during the collection of the geophysical and geological datasets in
560 2005 and 2006. We thank Robert Gatliff for comments on an earlier version of this manuscript,
561 which was further improved by the reviews of Robert Duck and Colm O’Cofaigh. Published with
562 the permission of the Executive Director, BGS (NERC).

563

564 **References**

- 565
- 566 AARSETH, I.A., LØNNE, O. & GISKEØDEGAARD, O. 1989. Submarine slides in glaciomarine
567 sediments in some western Norwegian fjords. *Marine Geology*, **88**, 1–21.
- 568 BALLANTYNE, C.K. 2002. Paraglacial geomorphology. *Quaternary Science Reviews*, **21**, 1935-
569 2017.
- 570 BRADWELL, T., FABEL, D., STOKER, M.S., MATHERS, H., MCHARGUE, L. & HOWE, J.A. 2008. Ice
571 caps existed throughout the Lateglacial Interstadial in northern Scotland. *Journal of*
572 *Quaternary Science*, **23**, 401–407.
- 573 BRYN, O., SOLHEIM, A., BERG, K., LIEN, R., FORSBERG, C.F., HAFLIDASON, H., OTTESEN, D. &
574 RISE, L. 2003. The Storegga Slide complex; repeated large scale sliding in response to climate
575 cyclicity. In LOCAT, J. & MIENERT, J. (eds) *Submarine Mass Movements and their*
576 *Consequences*, Kluwer Academic Publishing, Netherlands, 215–222.
- 577 CHURCH, M. & RYDER, J.M. 1972. Paraglacial sedimentation: a consideration of fluvial processes
578 conditioned by glaciation. *Geological Society of America, Bulletin*, **83**, 3059–3071.
- 579 COOK, H.E., FIELD, M.E. & GARDNER, J.V. 1982. Characteristics of Sediments on Modern and
580 Ancient Continental Slopes. In: SCHOLLE, P.A. & SPEARING, D. (eds) *Sandstone Depositional*
581 *Environments*. American Association of Petroleum Geologists, Tulsa, Oklahoma, 329–364.
- 582 EVANS, D., MCGIVERON, S., HARRISON, Z., BRYN, P. & BERG, K. 2002. Along-slope variation in
583 the late Neogene evolution of the mid-Norwegian margin in response to uplift and tectonism.
584 In DORÉ, A.G., CARTWRIGHT, J.A., STOKER, M.S., TURNER, J.P. & WHITE, N. (eds)
585 *Exhumation of the North Atlantic Margin: Timing, Mechanisms and Implications for*
586 *Petroleum Exploration*. Geological Society, London, Special Publications, **196**, 139–151.

587 FAIRBANKS, R.G., MORTLOCK, R.A., CHIU, T.C., KAPLAN, A., GUILDERSON, T.P., FAIRBANKS,
588 T.W. & BLOOM, A.L. 2005. Marine radiocarbon calibration curve spanning 0 to 50,000years
589 B.P. based on paired $^{230}\text{Th}/^{234}\text{U}/^{238}\text{U}$ and ^{14}C dates on pristine corals. *Quaternary Science*
590 *Reviews*, **24**, 1781–1796.

591 HAFLIDASON, H., SEJRUP, H.P., NYGÅRD, A., MIENERT, J., BRYN, P., LIEN, R., FORSBERG, C.F.,
592 BERG, K. & MASSON, D. 2004. The Storegga Slide: architecture, geometry and slide
593 development. *Marine Geology*, **213**, 201–234.

594 HAMILTON, E.L. 1985. Sound velocity as a function of depth in marine sediments. *Journal of the*
595 *Acoustic Society of America*, **78**, 1348–1355.

596 HAMPTON, M.A., LEE, H.J. & LOCAT, J. 1996. Submarine landslides. *Revue of Geophysics* **34**,
597 33-59.

598 HEATH, S., HASTINGS, T. & RAE, G. (eds). 2000. *Final Report of the Joint Government/Industry*
599 *Working Group on Infectious Salmon Anaemia (ISA) in Scotland*. Scottish Executive. 142pp.

600 HJELSTUEN, B.O., HAFLIDASON, H., SEJRUP, H.P. & LYSÅ, A. 2009. Sedimentary processes and
601 depositional environments in glaciated fjord systems – Evidence for Nordfjord, Norway.
602 *Marine Geology*, doi:10.1016/j.margeo.2008.11.010.

603 JENNER, K.A., PIPER, D.J.W., CAMPBELL, D.C. & MOSHER, D.C. 2007. Lithofacies and origin of
604 late Quaternary mass transport deposits in submarine canyons, central Scotian Slope, Canada.
605 *Sedimentology*, **54**, 19-38.

606 KNIGHT, J. 1999. Geological evidence for neotectonic activity during deglaciation of the southern
607 Sperrin Mountains, Northern Ireland. *Journal of Quaternary Science*, **14**, 45–57.

608 LEE, A.J. & RAMSTER, J.W. 1981. *Atlas of the Seas around the British Isles*. Ministry of
609 Agriculture, Fisheries and Food (MAFF). 90pp.

610 LOWE, D.R. 1982. Sediment gravity flows, II. Depositional models with special reference to the
611 deposits of high-density turbidity currents. *Journal of Sedimentary Petrology*, **52**, 279–297.

612 MCQUILLIN, R. & ARDUS, D.A. 1977. *Exploring the Geology of Shelf Seas*. Graham & Trotman,
613 London.

614 MIDDLETON, G.V. 1967. Experiments on density and turbidity currents, III. Deposition of
615 sediment. *Canadian Journal of Earth Science*, **4**, 475–505.

616 MULDER, T. & COCHONAT, P. 1996. Classification of offshore mass movements. *Journal of*
617 *Sedimentary Research*, **66**, 43–57.

618 MUSSON, R. 2003. *Seismicity and Earthquake Hazard in the UK*. British Geological Survey:
619 http://www.quakes.bgs.ac.uk/hazard/Hazard_UK.htm.

620 NARDIN, T.R., HEIN, F.J., GORSLINE, D.S. & EDWARDS, B.D. 1979. A review of mass movement
621 processes, sediment and acoustic characteristics, and contrasts in slope and base-of-slope
622 systems versus canyon-fan-basin floor systems. *Society of Economic Palaeontologists and*
623 *Mineralogists Special Publication*, **27**, 61–73.

624 NIESSEN, F. & WHITTINGTON, R.J. 1997. Synsedimentary faulting in an East Greenland Fjord. *In*
625 DAVIES, T.A., BELL, T., COOPER, A.K., JOSENHANS, H., POLYAK, L., SOLHEIM, A., STOKER,
626 M.S. & STRAVERS, J.A. (eds) *Glaciated Continental Margins: An Atlas of Acoustic Images*,
627 Chapman & Hall, London, 130–131.

628 OLESEN, O., BUNGUM, H., DEHLS, J., LINDHOLM, C., PASCAL, C. & ROBERTS, D. 2008.
629 Neotectonics in Norway – mechanisms and implications. Abstract: International Geological
630 Congress, Oslo, 2008. Available at: <http://www.cprm.gov.br/33IGC/1398408.html>.

631 PICKERING, K., HISCOTT, R. & HEIN, F. 1989. *Deep-marine environments: clastic sedimentation*
632 *and tectonics*. Unwin Hyman Ltd, London, 416pp.

633 POWELL, R.D. 2005. Subaquatic Landsystems: Fjords. *In*: Evans, D.J.A. (ed) *Glacial*
634 *Landsystems*. Hodder Arnold, London, 313–347.

635 RINGROSE, P.S. 1989. Palaeoseismic (?) liquefaction event in late Quaternary lake sediment at
636 Glen Roy, Scotland. *Terra Nova*, **1**, 57–62.

637 SEPA. 2006. *Designated Shellfish Waters in Scotland : Site Data. 61 Little Loch Broom*. Scottish
638 Environmental Protection Agency. 4pp.

639 SHANMUGAN, G. 1996. The Bouma Sequence and the turbidite mind set. *Earth Science Reviews*,
640 **42**, 201–229.

641 STEWART, I.S., FIRTH, C.R., RUST, D.J., COLLINS, P.E.F. & FIRTH, J.A. 2001. Postglacial fault
642 movement and palaeoseismicity in western Scotland: A reappraisal of the Kinloch Hourn
643 fault, Kintail. *Journal of Seismology*, **5**, 307–328.

644 STOKER, M.S. & BRADWELL, T. 2009. Neotectonic deformation in a Scottish fjord, Loch Broom,
645 NW Scotland. *Scottish Journal of Geology*, in press.

646 STOKER, M.S., LESLIE, A.B., SCOTT, W.D., BRIDEN, J.C., HINE, N.M., HARLAND, R., WILKINSON,
647 I.P., EVANS, D. & ARDUS, D.A. 1994. A record of late Cenozoic stratigraphy, sedimentation
648 and climate change from the Hebrides Slope, NE Atlantic Ocean. *Journal of the Geological*
649 *Society, London*, **151**, 235–249.

650 STOKER, M.S., BRADWELL, T., WILSON, C.K., HARPER, C., SMITH, D. & BRETT, D. 2006. Pristine
651 fjord landsystem revealed on the sea bed in the Summer Isles region, NW Scotland. *Scottish*
652 *Journal of Geology*, **42**, 89-99.

653 STOKER, M.S., BRADWELL, T., HOWE, J.A., WILKINSON, I.P. & MCINTYRE, K. In press.
654 Lateglacial ice-cap dynamics in NW Scotland: evidence from the fjords of the Summer Isles
655 region. *Quaternary Science Reviews*.

- 656 SYVITSKI, J.P.M. 1989. On the deposition of sediment within glacier-influenced fjords:
657 oceanographic controls. *Marine Geology* **85**, 301-329.
- 658 SYVITSKI, J.P.M. & HEIN, F.J. 1991. *Sedimentology of an Arctic Basin: Itirbilung Fiord, Baffin*
659 *Island, Northwest Territories*. Geological Survey of Canada Paper 91-11.
- 660 SYVITSKI, J.P.M. & SHAW, J. 1995. Sedimentology and Geomorphology of Fjords. In Perillo,
661 G.M.E. (ed) *Geomorphology and Sedimentology of Estuaries. Developments in*
662 *Sedimentology 53*, Elsevier Science BV, Amsterdam, 113–178.
- 663 WHITTINGTON, R.J. & NIESSEN, F. 1997. Staircase rotational slides in an ice-proximal fjord
664 setting, East Greenland. In DAVIES, T.A., BELL, T., COOPER, A.K., JOSEPHANS, H., POLYAK,
665 L., SOLHEIM, A., STOKER, M.S. & STRAVERS, J.A. (eds) *Glaciated Continental Margins: An*
666 *Atlas of Acoustic Images*, Chapman & Hall, London, 132–133.
- 667

668 **Table captions**

669 1. Interpretation of Late Quaternary stratigraphic units in the Summer Isles region (after Stoker
670 *et al.* in press).

671 2. Summary of stratigraphy and lithofacies proved in SAMS and BGS cores in Little Loch
672 Broom. SAMS cores prefixed by GC; BGS core prefixed by 57-06.

673 3. Summary of characteristics of mass failure and mass transport deposits in Little Loch Broom.

674

675 **Figure captions**

676 1. Location of study area, which is expanded in Fig. 4, in relation to the regional structural
677 grain. Occurrences of all areas of mass failure cited in text are shown. Abbreviations: A,
678 Ardessie debris lobe; B, Badcaul Slide; C, Cadail Slide; LB, rotational slumping in Loch
679 Broom; LLB, Little Loch Broom Slide Complex.

680 2. Late Quaternary stratigraphic scheme for the Summer Isles region (simplified from Stoker *et*
681 *al.* in press), including inferred relative timing of neotectonic events.

682 3. Geoseismic profiles showing distribution of Quaternary units, major zones of sliding, and
683 location of sediment cores (used in this study). a) Slope-parallel profile on northern flank of
684 outer Little Loch Broom; b) axial profile along length of Little Loch Broom, with seismic
685 inset showing sub-bottom detail of the Rireavach Slide, and relationship to pre-slide
686 stratigraphy. Profiles are located in Fig. 4. 1–3, main slide scars associated with Rireavach
687 Slide. Abbreviations: BT, bottom tracking indicator; IR, internal reflector in disturbed
688 section; P, pockmark; SBM, sea bed multiple.

- 689 4. Swath bathymetric image of Little Loch Broom showing: 1) the location of the enlarged
690 panels in Figs 5 & 7; 2) the location of the geoseismic profiles in Fig. 3; and, 3) the location
691 and summary lithology logs of the SAMS and BGS cores used in this study.
- 692 5. a) Detailed swath bathymetric image of the Little Loch Broom Slide Complex, showing the
693 distribution of the component slides and mass transport deposits (see Fig. 4 for location).
694 Abbreviations: ER, eastern re-entrant; NR, northern re-entrant. 1–3, slide scars of Rireavach
695 Slide. b) Perspective view of Ardessie debris lobe, looking SE within inner Little Loch
696 Broom (see Fig. 4 for location). Seismic inset shows sub-bottom detail of the debris lobe
697 (base = yellow reflector) and relationship to Summer Isles Formation (base = red reflector).
- 698 6. Core photographs of mass transport deposits: a) core GC087 from Rireavach Member
699 (Rireavach Slide) showing sharp, discordant contact between sandy mud and dipping
700 laminated clay (1.24–1.68 m); b) core GC092 from Late-stage debris flow unit (Badcaul
701 Slide) showing recumbent, isoclinal folding of sand beds (1.61–2.05 m). Abbreviation: A,
702 artefact – caused by sweep of osmotic knife during cleaning of surface of core; c) core
703 GC088 from Summer Isles Formation showing recumbent, isoclinally-folded laminated clay
704 sharply bounded, above and below, by basinal silty clay (2.16–2.8 m).
7. Detailed swath bathymetric image (a) and seismic profile (b) showing the Badcaul Slide on
the inner part of the mid-loch sill. The seismic profile shows the disposition of the Late
Quaternary units, in particular the disturbed Assynt Glacigenic Formation, and the Late-stage
debris flow unit at the base of the slope, sandwiched between the Annat Bay and the Summer
Isles formations. Lower seismic inset in (b) shows detail of Late-stage debris flow unit; upper
seismic inset shows evidence of rotational sliding (slumping) in the Assynt Glacigenic
Formation. Abbreviations: BT, bottom tracking indicator; SBM, sea bed multiple.

Table 1

Stratigraphic unit	Depositional setting
Summer Isles Fm	Marine deposits strongly influenced by bottom currents. Localised mass failure
Ullapool Gravel Fm	Fluvioglacial outwash fan-deltas
Inner and Outer Loch Broom shell beds	Time-transgressive condensed section in Loch Broom
Late-stage debris flows	Discrete, localised debris-flow deposits
Annat Bay Fm	Distal glacial marine facies, diachronous with Assynt Glacigenic Fm
Assynt Glacigenic Fm (including Rireavach Member in Little Loch Broom and other Late-stage members in Loch Broom)	Recessional, oscillating, ice-contact and proximal glacial marine facies. Contemporaneous mass failure, e.g. Little Loch Broom slide complex; Cadail slide (pre-Annat Bay Fm); neotectonic deformation in Loch Broom
Loch Broom Till Fm	Subglacial lodgement till

Table 2

Stratigraphy	Cores	Lithofacies description
<i>HOLOCENE</i>		
Holocene lag (Outer Little Loch Broom)	GC087 GC093 GC112/113 GC115 GC119 GC120 GC122/57-06/286	Predominantly grey, dark grey and olive grey, very poorly sorted muddy, very fine-grained sand and sandy mud, with gravel clasts and shells/shell fragments, including <i>Turritella</i> sp. and paired bivalves, commonly concentrated at the base of the unit. In core GC120, muddy sandy gravel bed crops out at sea bed. In core GC122, fine- to coarse-grained muddy sand is predominant with abundant shells at the base of the unit.
Summer Isles Formation (Inner Little Loch Broom)	GC092 GC088	Dark to very dark greenish grey, homogeneous, massive, mottled (bioturbated), soft and sticky, organic-rich silty to slightly silty clay, with sporadic fine- to medium-grained sand grains and shells/shell fragments. Core GC088 preserves a discrete slumped bed, 0.43 m thick, of greenish grey laminated clay bounded by homogeneous clay. In core GC092, base of core is slightly sandy and mottled through bioturbation.
<i>LATEGLACIAL</i>		
Late-stage debris flow (Lithogenetic unit)	GC092	Interbedded dark olive-grey homogeneous silty clay and greyish brown, muddy, very fine- to fine-grained sand, with scattered shells/shell fragments. Sandy beds are 1.5–4.0 cm thick, and display tight isoclinal folding.
Rireavach Member (Assynt Glacigenic Fm)	GC122 57-06/286 GC119 GC087	Reddish brown, massive, compact, medium- to coarse-grained, gravelly (granule grade) sand dominated by quartz and lithics; very poorly sorted, with sporadic shell fragments. Top of sand is reworked by Holocene lag. 0.2 m-thick bed of dark grey to grey, very fine- to fine-grained sand, moderately sorted with shells/shell fragments; on, 0.69 m of dark grey to grey, slightly sandy clay with abundant shells/shell fragments, and patches of lithic grains (intraclasts?). 0.62 m-thick bed of colour laminated (grey, dark greenish grey, pale red and dark greyish brown) silty clay, with inclined and disrupted lamination; on, 0.14 m-thick bed of grey sandy mud that includes abundant intact and comminuted shells, and subangular lithic clasts; on, homogeneous pale grey clay, becoming dark grey-brown and slightly silty towards the base.
Assynt Glacigenic Formation (Pre-slide deposits)	GC093 GC112 GC113 GC115 GC120	Homogeneous to colour laminated (dark grey to brown, greyish brown and reddish grey), soft and buttery, clay and silty clay. Laminae range from 0.5–1.5 cm. Bioturbation and reduction spots locally observed. Common pebbles (up to 2 cm) and shells/shell fragments, and sporadic very thin to thin beds (2–12 cm) of reddish grey, fine- to coarse-grained muddy sand.

Table 3

Stratigraphy	Indicator of instability	Morphology – swath and seismic characteristics	Sedimentary structures	Mass transport process
<i>HOLOCENE</i>				
Summer Isles Formation	Ardessie debris lobe	Base of slope lobe(s); hummocky sea bed; structureless internal reflection pattern; sourced by several slope gullies	No data	Mass flow
	Core GC088	Seismically unresolvable bed within parallel bedded sequence	Recumbent, isoclinally-folded clay bed; sharp upper and lower bed contacts	Slide
<i>LATEGLACIAL</i>				
Late-stage debris flow (Lithogenetic unit)	Badcaul Slide & core GC092	Irregular, hummocky sea bed; series of terraces backed by scalloped headwall scarps; sub-planar and curved, concave-up slide surfaces; bedding locally rotated into slide surface; mounded, lensoid lobe at base of slope with structureless to irregular internal reflection pattern	Recumbent, isoclinally-folded interbeds of sand and silty clay; sharp bounding bed contacts	Slide and mass flow
Rireavach Member (Assynt Glacigenic Fm)	Little Loch Broom Slide Complex Rireavach Slide & core GC087 Carnach Slide & core GC119 Scoraig Slide Corran Scoraig debris lobes & cores GC122 & 57-06/286	Irregular, hummocky sea bed bounded by several discrete scarps, including multiple scarps and terraces of Rireavach Slide; scalloped to rectilinear slide scars; sub-planar and curved concave-up slide surfaces; stacked, lensoid lobes on lower slope and basin floor; mainly structureless to chaotic internal reflection pattern	Highly variable lithofacies, including dipping laminated clay, massive gravelly sand, mud with matrix-supported clasts, and thin-bedded shelly gravelly sand; bed contacts are sharp	Slide and mass flow

Fig 1

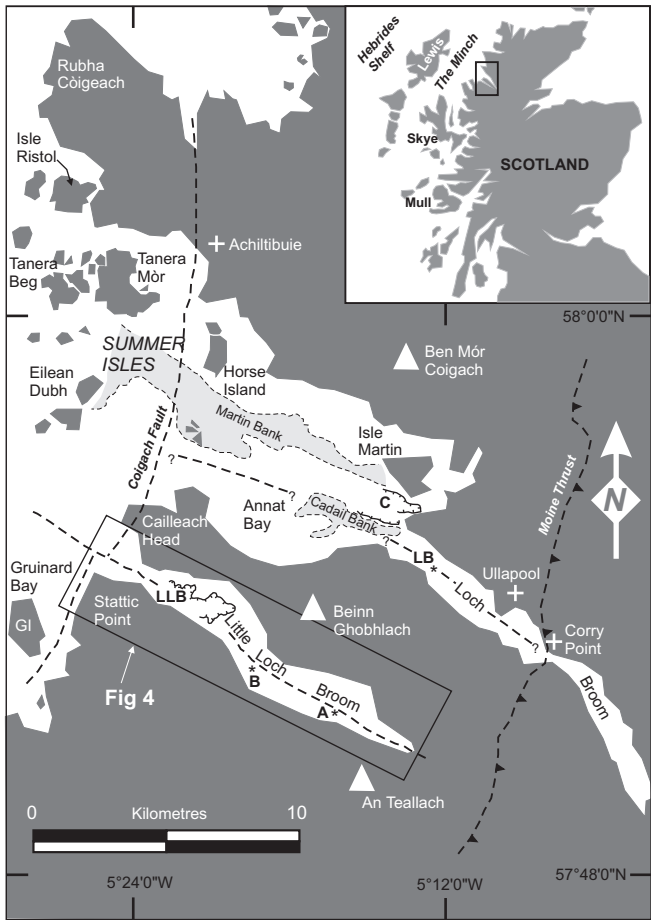


Fig 2

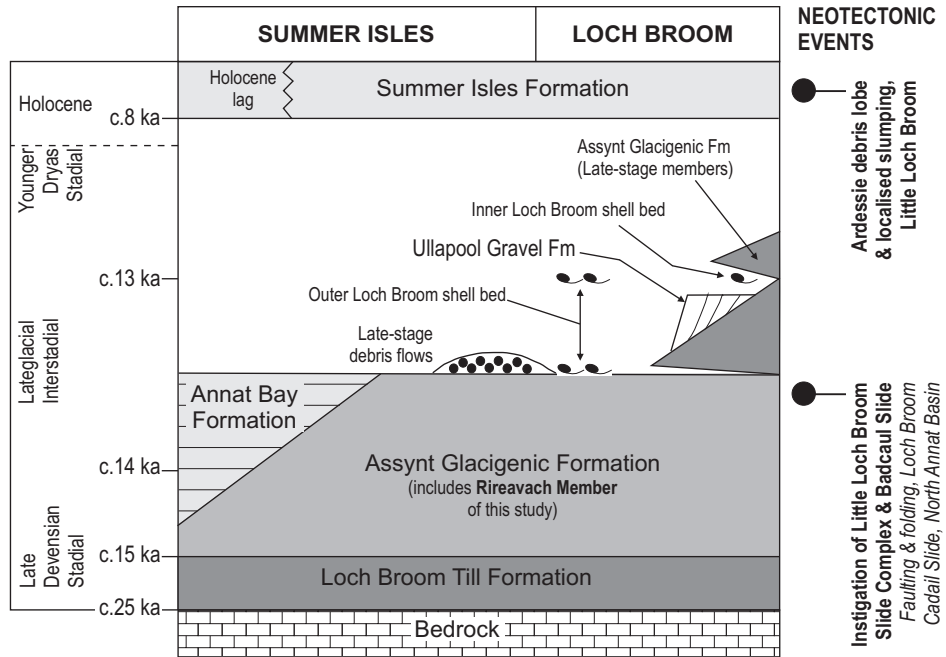


Fig 3

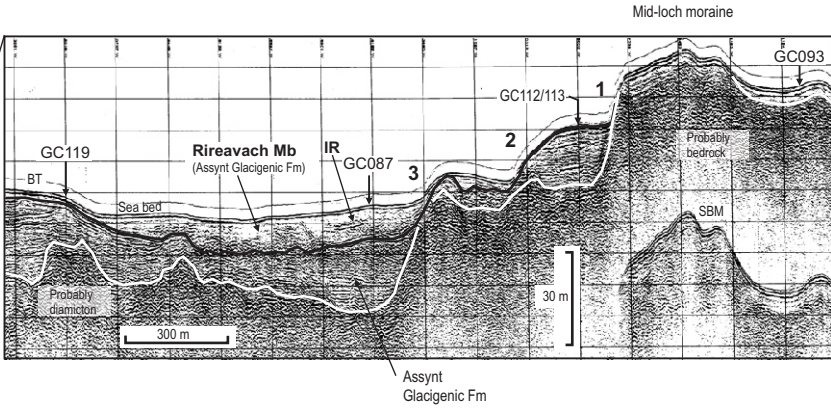
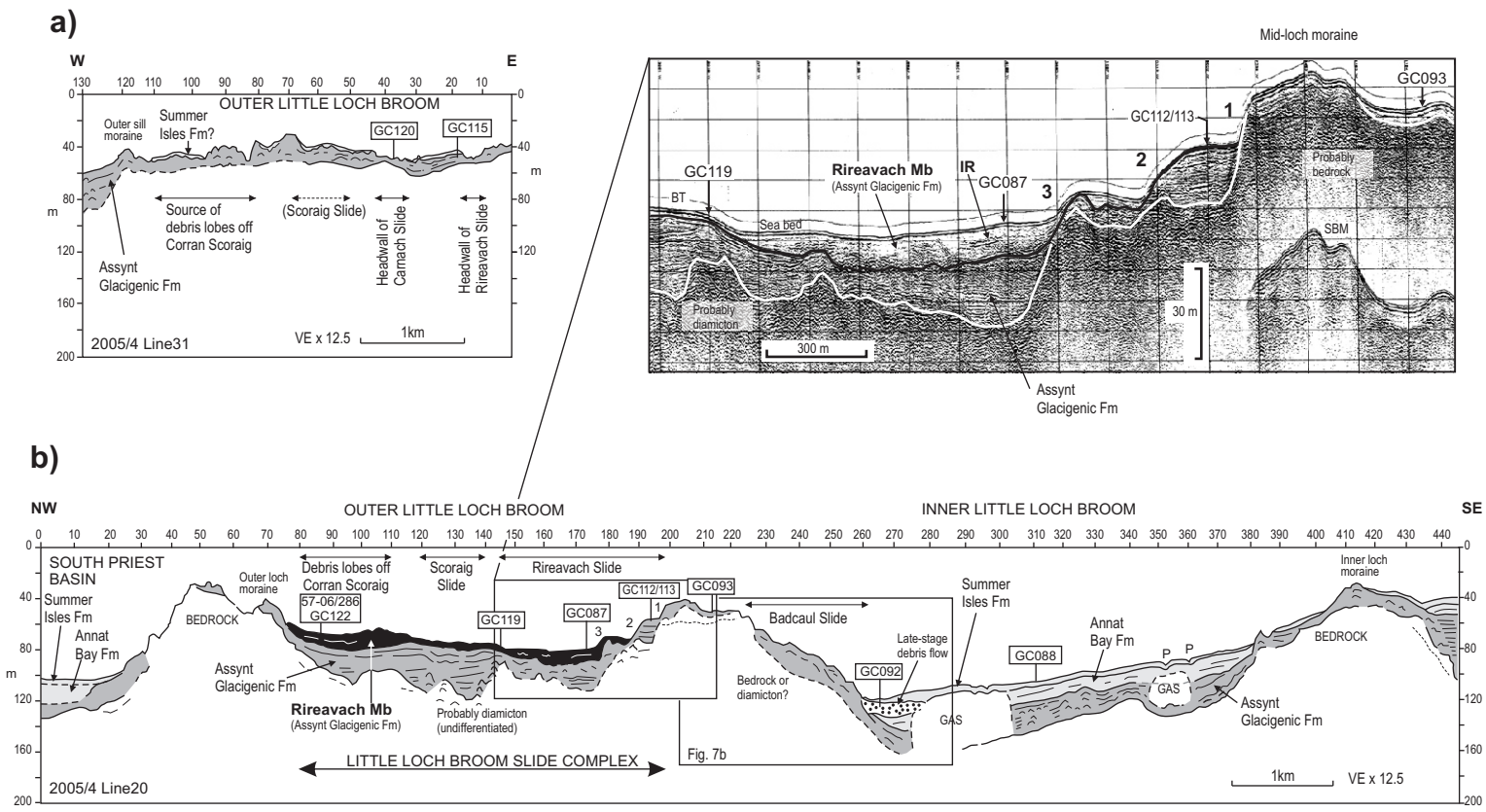


Fig 4

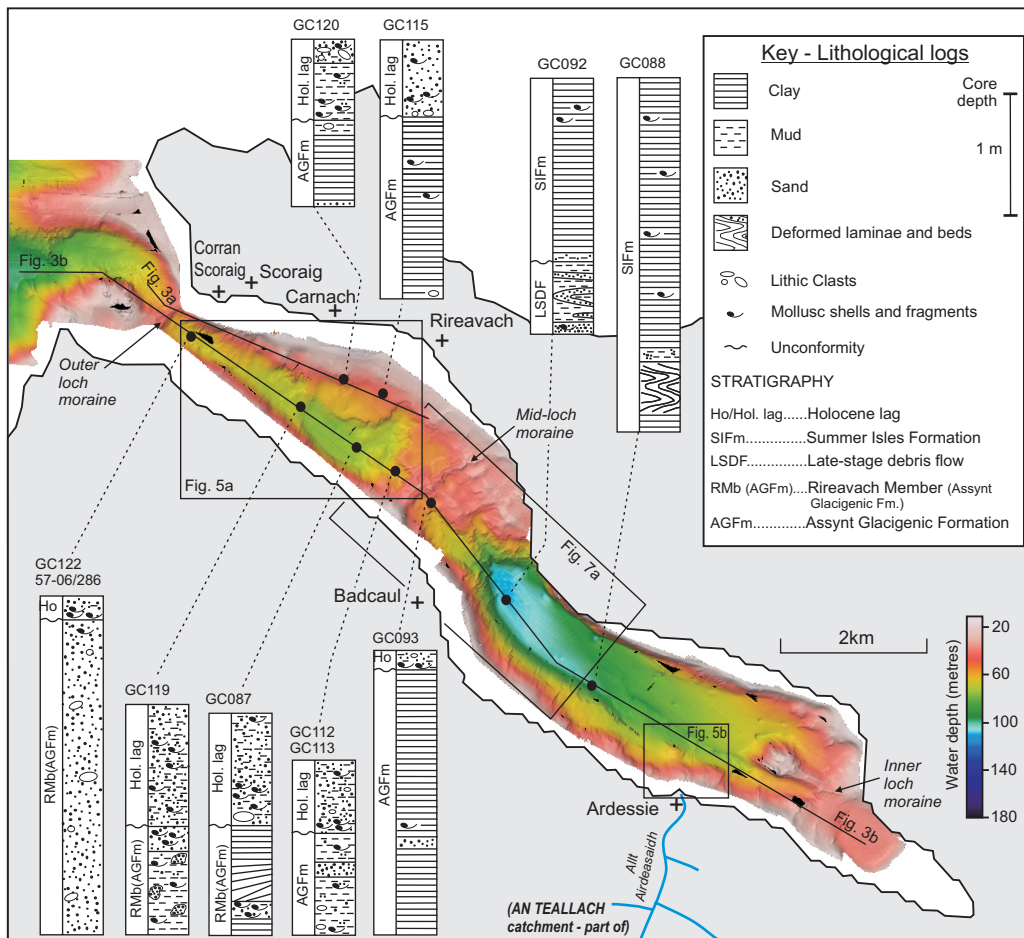


Fig 5

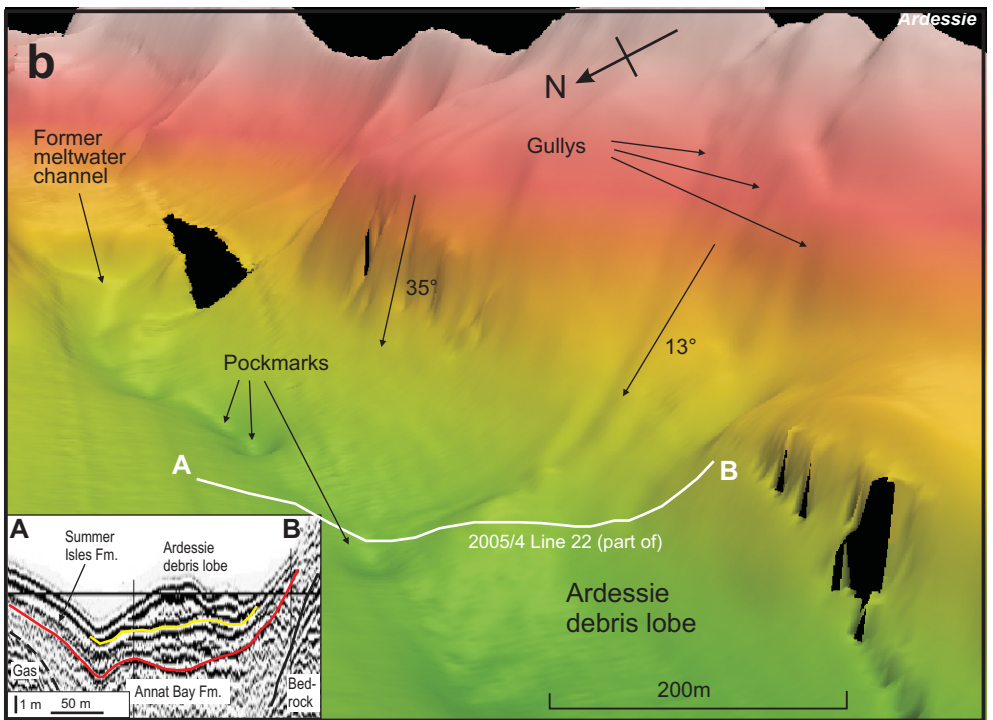
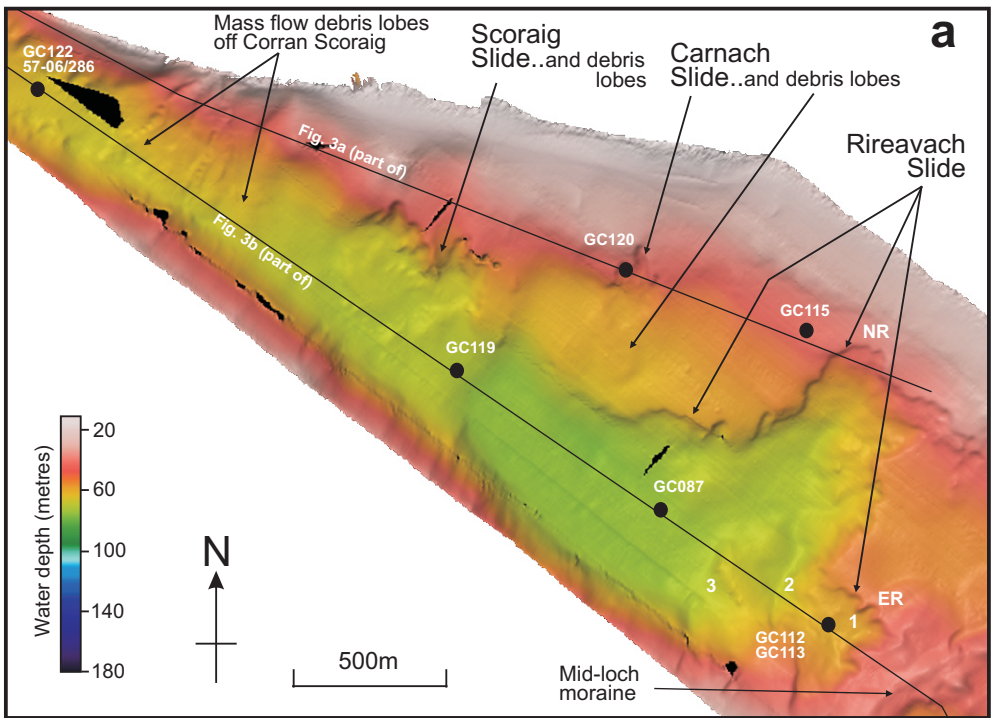
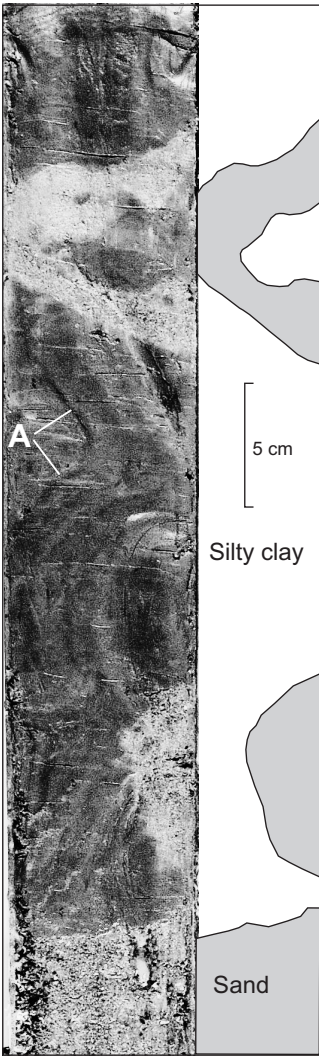


Fig 6

a) GC087



b) GC092



c) GC088

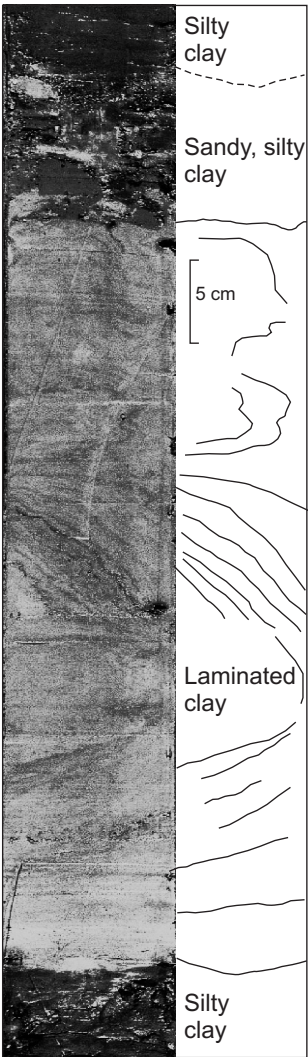


Fig 7

